RESEARCH PAPER

SEASONAL CHARACTERISTICS OF LONG-RANGE TRANSPORT AND POTENTIAL ASSOCIATED SOURCES OF PARTICULATE MATTER (PM_{10}) POLLUTION AT THE STATION ELK, POLAND, ON 2021-2022 DATA

Sheyar Abdo[1,2*], Yulia Koroleva[1]

[1]Immanuel Kant Baltic Federal University, Institute of Living Systems, Universitetskaya 2, Kaliningrad, 236041, Russia

[2]Tishreen University, Faculty of Literature and Humanities, Geography Department, Latakia, Syria

***Corresponding author:** abdosheyar@gmail.com

Received: May 26th, 2022 / Accepted: September 4th, 2023 / Published: October 10th, 2023

https://DOI-10.24057/2071-9388-2022-2461

ABSTRACT. The current study aimed to determine the potential sources of distant emissions of PM_{10} particles that significantly affect PM_{10} levels at a given site in southeastern Baltic. The EEA Air Quality Monitoring Station in Elk City, northeastern Poland, was selected for this study. This station is located approximately 50 km from the border of the Russian exclave (Kaliningrad Region). In this study, the NOAA HYSPLIT_4 trajectory model, potential source contribution function (PSCF), and concentration-weight trajectory (CWT) were employed to investigate the origin of the measured PM_{10} mass at a receptor site. PSCF and CWT utilize back-trajectory analysis and Lagrangian particle dispersion simulations to reconstruct the advection pathways of air masses arriving at the site. These reconstructed retroplumes provide detailed information regarding the geographic locations traversed by polluted air masses on their way to the receptor. By integrating trajectory information with concurrent pollutant concentration data, the PSCF and CWT enable the identification of potential source regions and quantification of their impact on the observed atmospheric levels. From January 1, 2021, to December 31, 2022, at 200 m the 72h backward trajectories of air masses entering the receptor point were calculated and categorized by clustering them into 5-4-4-5 clusters. Subsequently, the PM_{10} levels at the Elk site associated with each air mass cluster were examined during the observation period. The seasonal variation in PM_{10} was generally characterized by a peak in winter and minimum values in summer. PM_{10} was lower during warmer periods, particularly during summer, and significantly, higher concentrations were observed during colder periods. Cluster analyses showed that airflow followed a seasonal pattern, with different results obtained in different seasons. According to the PSCF and CWT results, in winter and spring, the receptor site was influenced more by long-range PM_{10} pollution, particularly from heavily industrialized areas in Central-Eastern Europe. In contrast, in summer and autumn, the receptor site was less influenced by long-range pollution. The findings demonstrate that the seasonal distributions of PM_{10} source areas obtained using these two methods generally share similar characteristics, suggesting the credibility and accuracy of the analytical results.

KEYWORDS: pollution sources; PM_{10}; HYSPLIT; backward trajectory; potential source contribution function; concentration-weighted trajectory

CITATION: Abdo S., Koroleva Y. (2023). Seasonal Characteristics Of Long-Range Transport And Potential Associated Sources Of Particulate Matter (Pm_{10}) Pollution At The Station Elk, Poland, On 2021-2022 Data. Geography, Environment, Sustainability, 3(16), 92-101

https://DOI-10.24057/2071-9388-2022-2461

ACKNOWLEDGEMENTS: The authors express their gratitude to the Elk station team and European Union (EU) Environment Agency for providing air pollution data without charge. The authors also thank NOAA's Air Resources Laboratory (ARL) for providing the HYSPLIT transport and dispersion model used in this paper. We also gratefully thank the reviewers for their constructive comments.

Conflict of interests: The authors reported no potential conflict of interest.

INTRODUCTION

Today's atmosphere differs significantly in terms of its chemical composition from the natural atmosphere that existed before the Industrial Revolution. If the natural atmosphere is considered clean, it means that in today's atmosphere, clean air is never found (Daly and Zanetty, 2007). The history of air pollution dates back centuries, when the industrial revolution (circa 1760) was a major contributor to the issue, as the widespread use of fossil fuels has led to the release of large quantities of pollutants, such as sulfur dioxide, nitrogen oxides, and particulate matter into the atmosphere (Kim, 2013; Yang and Smintek, 2014). In the twenty-first century, one of the biggest challenges was air pollution, not only at the global scale but also at the local and regional levels. Particulate matter (PM) is one of the main pollutants of concern because of its negative impacts on ecosystems and human health, as exposure to PM can cause a range of health problems, including premature death, cardiovascular and respiratory diseases, and reduced lung function (Manisalidis et al., 2020).

The southern Baltic is a geographically diverse region with a various disparities in areas such as economic development, climate type, landform, and resource endowment. These disparities have resulted in large differences in pollutant and PM levels in the region. While the Baltic States and Kaliningrad region have relatively low levels of PM, Poland frequently experiences PM pollution levels that exceed the limits recommended by the WHO. According to a report by the European Environment Agency (EEA) published in 2021, Poland had the highest average annual concentration of PM2.5, with levels exceeding the EU's recommended limit of 10 μg/m^3 and the second-highest average annual concentration of PM_{10} in Europe, with levels exceeding the EU's recommended limit of 20 μg/m^3.

The main sources of PM in Poland can be attributed primarily to coal-fired power plants, industrial emissions, and residential heating using solid fuels such as coal and wood. Open burning of agricultural waste is also a common practice in Poland, which releases large amounts of PM into the air that can also be transported over long distances (Jasiński et al., 2021; Kobza et al., 2018). In addition to this local sources, Long-range transport is another major source of PM pollution in Poland due to its geographical location in the center of Europe and its proximity to industrialized countries such as Germany, the Czech Republic, and Ukraine, which contribute to the high levels of PM pollution due to the prevailing westerly winds that carry pollutants from these countries to Poland (Nazar and Niedoszitko, 2022; Zareba and Danek, 2022).

Various computational approaches have been used to solve long-range pollutant transport. Air mass back-trajectory analysis is frequently used to determine the direction and sources of air pollution at a receptor site. The basic idea behind air mass back-trajectory analysis is that the air masses that reach a receptor site have traveled through the atmosphere and may have picked up pollutants along the way. By analyzing back trajectories, scientists can gain insights into the sources of air pollution, the transport of pollutants across different regions, and the potential impacts of pollution on human health and the environment. Back trajectories are often used in conjunction with other atmospheric modeling tools, such as receptor models, to provide a more complete understanding of air pollution dynamics (Bodor et al., 2020; Pouyaei et al., 2020; Stein et al., 2015).

Several studies have used back trajectory analysis to investigate the long-range transport of air pollution; However, there is a lack of studies of air mass back-trajectories for south eastern Baltic region. In scarce previous studies performed for this region, potential sources of particulate matter (PM_{10}) were identified using cluster trajectory analysis and the concentration-weighted trajectory (CWT) approach at a rural background site in northeastern Poland (Diabla Góra) (Reiser and Orza, 2018). Backward trajectory analysis was also performed to identify the main atmospheric pathways affecting PM_{10} concentrations at urban background sites in Warsaw, Poland (Majewski et al., 2018). Another study by Bihałowicz et al., (2021) used backward trajectory analysis to study the dispersion of selected air pollutants and greenhouse gases from landfill fires and their impact on air quality in Poland. At the regional level, several studies have been conducted, the most important of which was a study conducted by Byčenkiene et al., (2014) to investigate the transport pathways and potential sources of Black Carbon (BC) and aerosol particle number concentration (PNC) observed in Lithuania.

The objective of this study is to investigate the potential source region of air pollution contributing to PM_{10} levels in an urban background location in northeastern Poland (Elk) based on back-trajectories and PM_{10} observations for 2021-2022. Elk station is located approximately 50 km away from the border of the Russian enclave (Kaliningrad Region). Therefore, this study can also provide an overview of the characteristics of PM_{10} pollution in the region, as no such observations have been carried out in the Kaliningrad region. Cluster analysis of back trajectories was used to assess the main transport pathways of air masses, whereas a hybrid receptor model as a function of the potential source contribution function (PSCF) and concentration-weighted trajectory (CWT) was used to identify potential PM_{10} source areas.

MATERIALS AND METHODS

Study Area and Data Sources

In this study, air mass back-trajectories arriving at a monitoring site in Elk, Poland were investigated. Elk is an urban background monitoring site operated within the EEA air quality network (European Environment Agency). This site is located in the north-eastern part of Poland, in the Warmian-Masurian Voivodeship (53°49'17"N 22°21'44"E, 133 m.a.s.l.).

Regional or mesoscale transport distances are consistently within 1000 km for about 2 to 3 days in the boundary layer (Li et al., 2012). As a result, we chose a 72-hour backward trajectory with 72 latitude-longitude data pairs per trajectory. Eight back trajectories were calculated at an altitude of 200 m above the ground starting point at 02:00, 05:00, 08:00, 11:00, 14:00, 17:00, 20:00, and 23:00 LT. The following are the reasons for selecting 200 m agl as the receptor height: First, PM_{10} concentrations are often measured below the surface layer, typically at a height of 200 m agl, where pollutants are well mixed. Second, when computing the backward trajectory, both the horizontal and vertical advections were considered. Air masses from higher or lower altitudes can reach a receiving height of 200 m agl (Bari et al., 2003; Zhu et al., 2011). The NCEP Global Forecast System (GFS) with a resolution (0.25x0.25 degree) offered daily meteorological data, which could be downloaded from the HYSPLIT website (https://www.ready.noaa.gov/archives.php). Hourly PM_{10} concentrations for receptor site during the period from January 1, 2021, to December 31, 2022, were obtained from the European Environment Agency Platform. Data are available at (https://discomap.eea.europa.eu/map/fme/AirQualityExport.htm/).

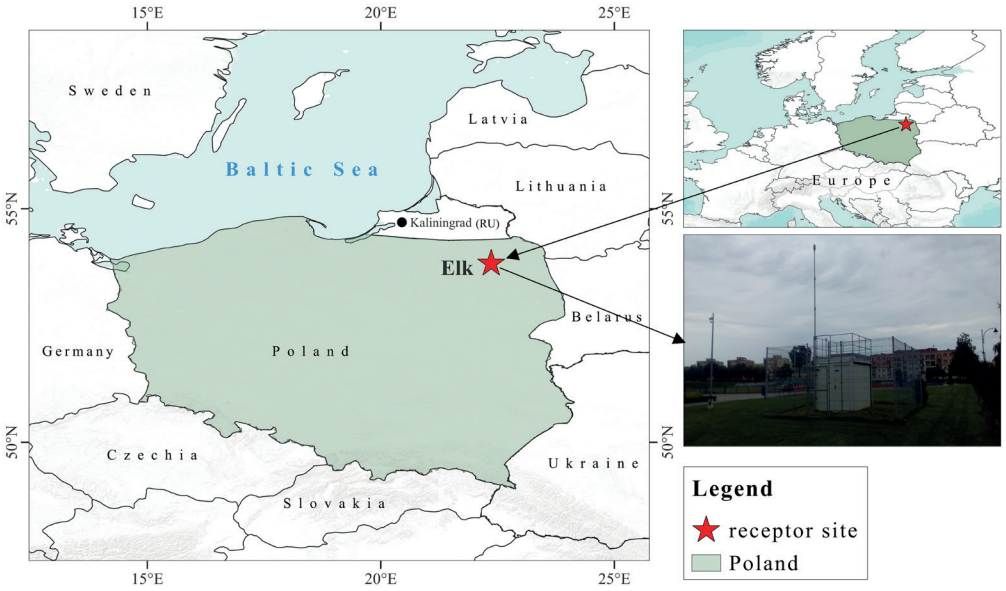

Fig. 1. The location of the study area. The red star represents the receptor point, i.e., the arrival point for air masses

Trajectory Models

To determine the potential impact of cross-region wind transport on air pollutants' concentrations, Trajectory Models were used. In the 1940s, the first Trajectory Models were developed (Draxler and Hess, 1998; Stein et al., 2015). They can help identify areas with transboundary air pollution sources by using regional weather data and Lagrangian functions to reconstruct air parcel routes at specific locations and over selected time periods (Draxler and Hess, 1998). To analyze atmospheric transport, several trajectory models have been constructed. They can be used to investigate how the movement of the atmosphere forward or backward in time. Flexible Trajectory Model (FLEXTRA; Fleming et al., 2012) and the HYSPLIT trajectory model (Draxler and Hess, 1998) are two examples. They have been used for retrospective analyses or prediction of possible pollution sources or pollution points. These models are considered relatively efficient and effective tools for atmospheric transport and dispersion modeling, as they require less computational effort than more complex and computationally demanding models.

The HYSPLIT model is one of the most widely used models for trajectory analysis. It is a comprehensive system that can calculate everything from simple air packet trajectories to complicated propagation and deposition simulations (Yerramilli et al., 2012a). The National Oceanic and Atmospheric Administration's (NOAA) Air Resources Laboratory used HYSPLIT model to investigate the sources and pathways of air pollution (Heffter et al., 1975). The model provides high-precision and time-continuous simulation results and has been widely used in the study of migration and diffusion of various pollutants in different fields. The HYSPLIT model is divided into two parts: the backward transport model and the forward diffusion model, which address the source- and sink-related problems, respectively (Draxler and Hess, 1998; Li et al., 2020; Sahu et al., 2019).

Trajectory clustering analysis

Cluster analysis is a multivariate statistical technique that has become more popular in studies of air pollution. Clustering means that, according to the similarity principle, data objects with higher similarity can be divided into the same cluster, and data objects with higher heterogeneity can be divided into different clusters (Moody and Galloway, 2017; S. Wang et al., 2017). The trajectory data was divided into many classes or clusters using trajectory clustering analysis, a multivariate statistical analytic technique. Data in the same class or cluster share a higher degree of similarity, whereas those in different classes or clusters vary more significantly (Xin et al., 2016). This study uses TrajStat, a plugin of MeteoInfo (Wang et al., 2009); this plugin can view, query, and cluster trajectories and includes two clustering methods: Euclidean distance and angle distance. The angle distance clustering approach is utilized to cluster airflow trajectories since this study determines the direction from which air masses arrive at the site. The angle distance, which varies between 0 and π, is often used to define the mean angle between the two trajectories (Sirois and Bottenheim, 1995). The PM_{10} concentrations associated with backward trajectories were then compared in each cluster.

$$d_{12} = \frac{1}{n}\sum_{i=1}^{n}\cos^{-1}\left(0.5\frac{\left(A_i + B_i - C_i\right)}{\sqrt{A_i B_i}}\right) \quad (1)$$

$$A_i = \left(X_1(i) - X_o\right)^2 + \left(Y_1(i) - Y_o\right)^2 \quad (2)$$

$$B_i = \left(X_2(i) - X_o\right)^2 + \left(Y_2(i) - Y_o\right)^2 \quad (3)$$

$$C_i = \left(X_2(i) - X_1(i)\right)^2 + \left(Y_2(i) - Y_1(i)\right)^2 \quad (4)$$

where *n* is total duration of a trajectory, "d_{12} is the mean angle between the two backward trajectories, as seen from the trajectory origin point and the variables X_0 and Y_0 define as the position of the receptor site (backward trajectory origin point). X_1 (Y_1) and X_2 (Y_2) reference backward trajectories 1 and 2, respectively".

Potential source contribution function (PSCF)

The PSCF (Hopke et al., 1995) is a commonly used method for identifying regional sources that is based on the HYSPLIT model, which uses meteorological data in its analytic scheme to generate a probability field that may be used to determine source emission potential (C. Y. Hsu et al., 2019). PSCF is a conditional probability function that estimates the likelihood of a pollutant-laden air parcel arriving at a receptor site after passing through a specified upwind source area. A gridded i by j array is used to split the possible source region (Hopke et al., 1995). PSCF is often

applied to selecting concentrations exceeding a certain level to pinpoint sources having the potential to induce high concentrations at the site, and many criteria are suggested in the literature to choose such 'cut-off' values. In this study, the PSCF threshold for PM_{10} concentrations was set at the 90th percentile.

The PSCF value for the ijth cell is then defined as the following:

$$PSCF_{ij} = n_{ij}/N_{ij} \quad (5)$$

where N_{ij} is the number of trajectories that crossed in the ij^{th} grid during the study period and n_{ij} is the number of trajectories that arrived at a receptor site with pollutant concentrations exceeding a predefined criteria value (Hopke et al., 1995).

The PSCF value can be considered the conditional probability that analyte concentrations above the threshold level are related to air parcel passage through the ij^{th} cell during transport to the receptor location. That is, cells with high PSCF values are linked to the arrival of air parcels with analyte concentrations higher than the threshold value at the receptor location. These cells represent regions where the constituent has a 'high potential' contribution (Wang et al., 2006). Studies have demonstrated that great uncertainty exists in the calculated result when N_{ij} is extremely small (Dimitriou et al., 2021). To eliminate this uncertainty, an arbitrary weight function, W_{ij}, was applied when the number of endpoints in a particular cell was less than three times the average number of endpoints for each cell (Hopke et al., 1995).

$$WPSCF_{ij} = W_{ij} \times PSCF_{ij} \quad (6)$$

$$W_{ij} = \begin{cases} 1.00 & N_{ij} > 80 \\ 0.70 & 20 < N_{ij} \le 80 \\ 0.42 & 10 < N_{ij} \le 20 \\ 0.05 & 0 < N_{ij} \le 10 \end{cases} \quad (7)$$

Concentration weighted trajectory (CWT)

Because the PSCF method has difficulty distinguishing between strong and moderate pollution sources, the CWT method was used to estimate the relative importance of probable sources (Hsu et al., 2003). As previously stated, one shortcoming of the PSCF approach is that grid cells with sample concentrations that were either slightly higher or significantly higher than the threshold could have the same PSCF result. As a result, distinguishing between moderate and powerful sources may be challenging (Ma et al., 2019). To identify the sources in each grid, the concentration-weighted trajectory method (CWT) was applied with the aim of producing a geographical overview of possible emission areas within the study region (Hsu et al., 2003). CWT method is allow to reconstruct "potential sources" or more precisely spatial distribution of mean contribution of potential sources to content of admixture in a receptor point (Shukurov and Shukurova, 2017). The calculation formula of the CWT method is given as follows (Hsu et al., 2003):

$$CWT_{ij} = \frac{\sum_{K=1}^{N} C_k \tau_{ijk}}{\sum_{K=1}^{N} \tau_{ijk}} \quad (8)$$

where CWT_{ij} is mean contribution of potential sources located in ij-cell into concentration in receptor point; N is the total number of trajectories; k denotes a trajectory; Ck is the PM_{10} concentration of trajectory k when it passes through ij-cell, which can be calculated using the HYSPLIT model; and τ_{ijk} is the duration in which trajectory k stays in ij-cell. In addition, the CWT method causes great uncertainties, thus the weight coefficient W_{ij} is needed to reduce these uncertainties (Y. K. Hsu et al., 2003; Stohl, 1998). Similarly, W_{ij} is determined using Equation (7), and the introduction of the coefficient is as follows:

$$WCWT_{ij} = W_{ij} \times CWT_{ij} \quad (9)$$

In this study, the domain for the PSCF grid covers the longitudes of about 30°W-60°E and the latitudes of 30°–75°N and contained 16,200 grid cells of 0.5° × 0.5°.

RESULTS AND DISCUSSION

PM_{10} Pollution Characteristics

The average hourly variations in PM_{10} concentrations from January 2021 to December 2022 are shown in Figure 2, and the monthly and seasonal variations are shown in Figure 3. The PM_{10} annual average concentrations for 2021 and 2022 are 20.6 μg/m^3 and 19.6 μg/m^3, respectively, which is less than twice the EU standard (40 μg/m^3). In addition, the number of days the EU air quality standard was exceeded was 38 between January 1, 2021, and December 30, 2022 (the 24-hour standard was 50 μg/m^3). The particulate matter (PM_{10}) concentrations measured in Elk showed clear seasonal variations, with the highest average PM_{10} concentrations observed in the winter months. For the period January 1, 2021 to December 30, 2022, the highest PM_{10} concentrations of approximately 23.34 μg/m^3 are found in winter (December, January and February), followed by spring (March to May) with 22.31 μg/m^3. In contrast, the lowest concentrations were recorded in summer (June to August) and autumn (September to November) with only 17.68 μg/m^3 and 17.44 μg/m^3, respectively. This suggests that the higher PM_{10} concentrations in winter were due to increased PM_{10} emissions from human activities, such as burning fossil or renewable fuel during the heating season. The highest monthly concentration was in March (33 μg/m^3) and the lowest was in September (13.7 μg/m^3).

Transport Pathways

This section discusses potential pollutant transport pathways to the Elk Site based on the results of the clustering analysis of backward trajectories calculated at 02:00, 05:00, 08:00, 11:00, 14:00, 17:00, 20:00, and 23:00 (LT) every day from January 2021 to December 2022 (Fig. 4).

TrajStat was used to process the airflow data to obtain seasonal transport trajectories. However, it was impossible to determine the exact number of trajectories in different directions using these airflow trajectories. Therefore, the trajectories in winter, spring, summer, and autumn were integrated into 5-4-4-5 clusters according to the consistency of the temporal and spatial distribution of backward trajectories (Fig. 5). Backward clustering trajectories that exceed the 90th percentile threshold for PM_{10} concentrations are presented and defined as "high-polluted" trajectories, while backward clustering trajectories corresponding to concentrations below the 90th percentile threshold are defined as "low-polluted" low-polluting trajectories.

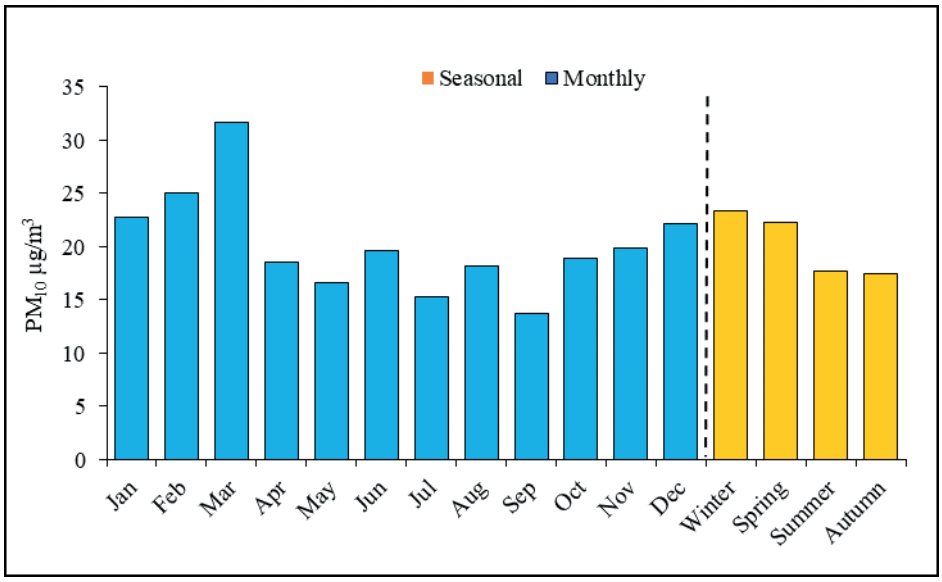

Fig. 2. Monthly and seasonal average PM_{10} variation at EEA station in the Elk city (Poland) from January 2021 to December 2022

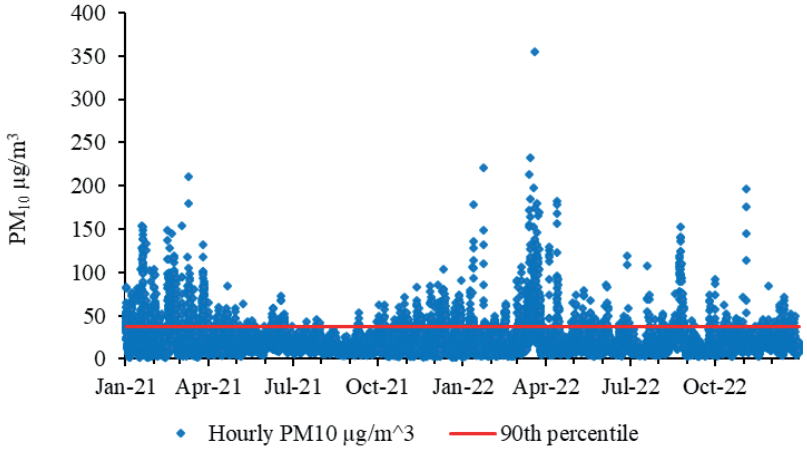

Fig. 3. Hourly average PM_{10} variation at EEA station in the Elk city (Poland) from 1 January 2021 to 31 December 2022

In winter, five clusters of backward trajectories were identified. The winter air flows were mainly from the west (cluster 4), accounting for 48.7% of the winter airflow. In spring, the backward trajectories were grouped into four clusters. Airflows from the northwest (cluster 4) accounted for the largest portion of airflows in spring at 33%, followed by the north (cluster 3) with 23.6% of airflows in spring. The airflows in summer were divided into four clusters. In summer, the airflows arriving at Elk have a divergent distribution. The western (cluster 4) and eastern airflows (cluster 3) had the largest shares of 43.8% and 28.9%, respectively. In autumn, there are five clusters of backward trajectories, the airflows are mostly western (cluster 3, accounts for 31% of the airflows in autumn), with longer transmission distances and faster speeds.

Based on the results of the clustering analysis of seasonal airflow backward, combined with the PM_{10} concentration data of Elk (Table 1), the potential impacts of various trajectories on PM_{10} levels in Elk were quantified. Consistent with the results discussed above, the PM_{10} concentration and number of polluted trajectories in winter and spring is higher than that in summer and autumn.

In winter, the airflows associated with clusters 3 and 5 are identified as the most polluted, with high levels of PM_{10} of 71.9 µg/m³ and 59.4 µg/m³, respectively. However, when considering the number of polluted trajectories, cluster 4, which is associated with the west airflow originating from the UK through the northern Netherlands and from Germany to western Poland, shows greater significance. Despite having a low PM_{10} concentration (approximately 51 µg/m³), cluster 4 had the highest number of pollution trajectories, which exceeded the threshold of 37.5 µg/m³. Specifically, it contributed to over 46% of the total winter-pollution trajectories. The high concentrations of PM_{10} may be related to the fact that these areas are in heating season, leading to increased anthropogenic emissions of pollutants, e.g., from the use of solid fuels for heating.

For spring, the highest average PM_{10} concentration for the polluted trajectories observed at the Elk site (74.9 µg/m³) was associated with the easterly airflow of cluster 2, which contributed 13.2% of the polluted trajectories in spring (Fig. 5b). High PM_{10} concentrations were also associated with northwesterly airflows (cluster 3), which contributed 41.9% of the pollution trajectories, with an average PM_{10} concentration of 66 µg/m³.

In summer, the average PM_{10} concentrations and the number of pollution trajectories associated with clusters were the least significant compared to the other seasons. In summer, many plants flourish, and the total leaf area of the surface vegetation significantly increases, which is conducive to the adsorption of atmospheric particulates (Indumali and Appuhamillage, 2018). The eastern airflow (cluster 2) was the most important in this season, as it accounted for more than 80% of the summer pollution trajectories, with an average PM_{10} concentration of 61.9 µg/m³.

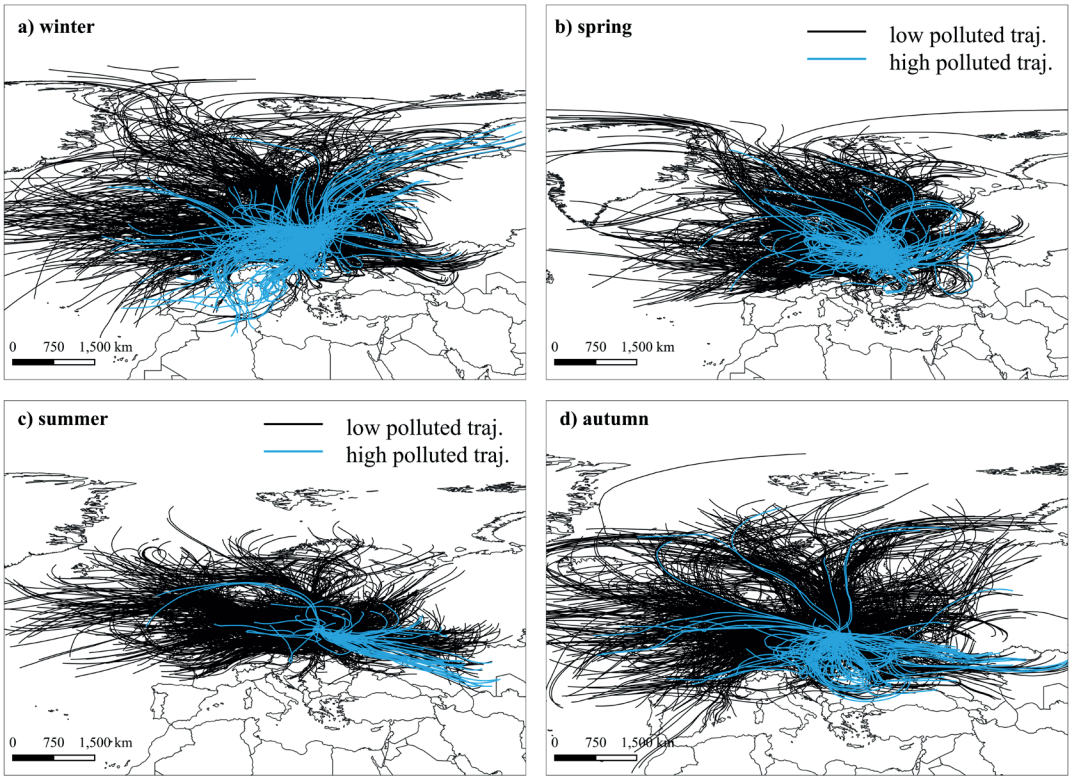

Fig. 4. 72-h backward trajectories for the four seasons (from January 2021 to December 2022); bold blue trajectories were identified as pollution trajectories (PM10 concentration >37.5 µg/m³).

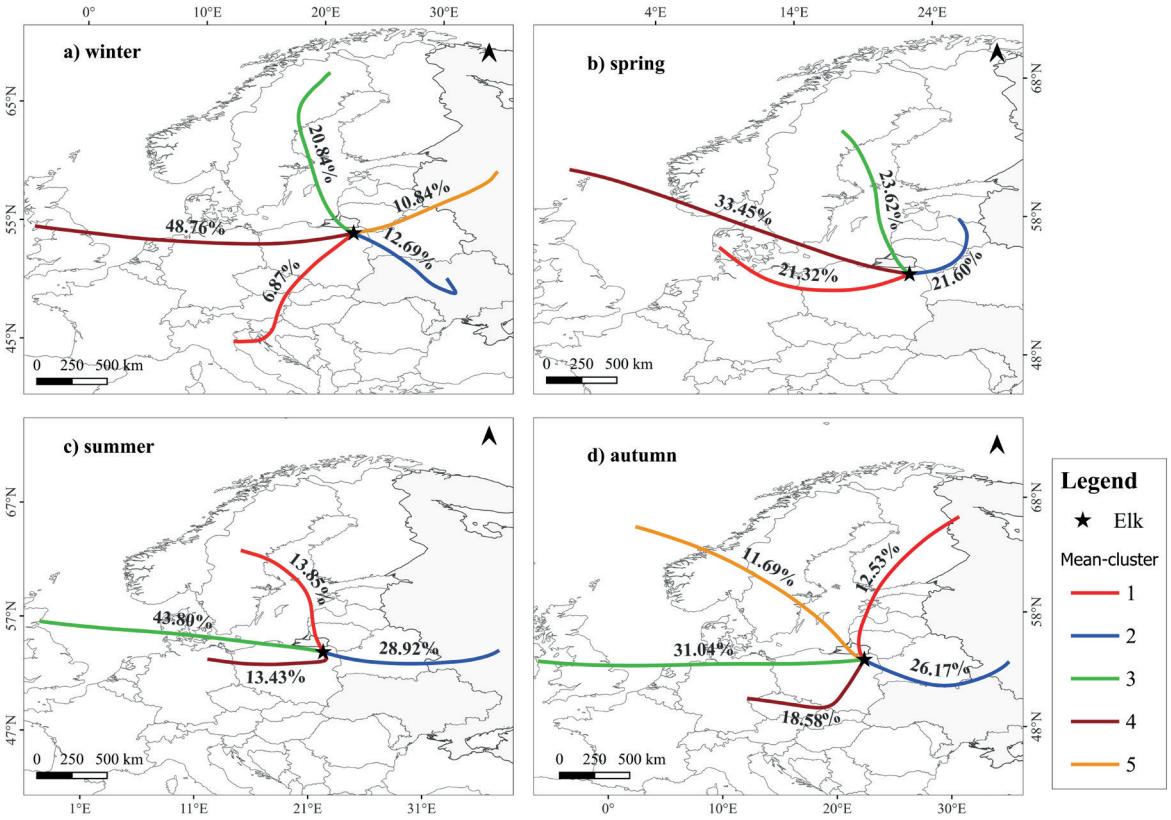

Fig. 5. Mean-Cluster backward trajectories at Elk site for the four seasons from January 2021 to December 2022

Table 1. Summary statistics of the cluster analysis showing the number of trajectories in each cluster and the mean concentration and standard deviation of PM_{10} concentrations.

Season	Cluster	All trajectories		Polluted trajectories	
		Number of traj.	Mean PM_{10} (μg/m³)	Number of traj.	Mean PM_{10} (μg/m³)
Winter	1	95	44.63±24.58	52	58.61±25.28
	2	177	28.38±13.85	30	50.85±18.24
	3	294	15.20±19.16	21	70.91±33.79
	4	683	22.12±16.21	114	51.27±12.22
	5	153	27.05±19.86	27	59.45±27.39
	All	1402	23.52±19.03	244	55.38±21.28
Spring	1	495	15.92±12.45	28	56.01±15.47
	2	336	17±19.05	23	74.92±33.94
	3	310	30.54±26.58	73	66.07±33.51
	4	317	25.11±21.36	50	59.60±33.51
	All	1458	21.28±20.50	174	63.76±31.67
Summer	1	204	12.13±8.10	4	48.11±14
	2	394	25.83±16.86	41	61.90±27.64
	3	630	11.95±5.65	2	56.80±17.49
	4	189	18.58±8.44	4	54.04±20.84
	All	1417	16.72±12.19	51	60.01±25.94
Autumn	1	180	10.02±7.58	2	54.40±6.92
	2	372	23.53±14.56	46	51.48±17.83
	3	443	16.77±13.75	16	60.60±42.98
	4	267	26.03±10.48	32	46.97±7.97
	5	162	12.10±10.24	3	64.39±20.81
	All	1424	18.89±13.62	99	51.95±21.99

In autumn, PM_{10} concentrations associated with western and northwestern airflows (clusters 3 and 5) were the highest (60.6 μg/m³, 64.4 μg/m³, respectively), but less significant in terms of the number of polluted trajectories. In contrast, eastern airflows were more significant (cluster 2), accounting for 46% of the total number of pollution trajectories in autumn, with an average PM_{10} concentration of 51.4 μg/m³.

Source analysis of PM10 based on PSCF and CWT methods

In order to fully reflect the long-range impact characteristics and contributions of potential source areas to PM_{10} mass concentrations in Elk, we conducted a potential source contribution function (WPSCF) analysis and a concentration-weighted trajectory (WCWT) analysis based on the backward trajectory of each season from 2021 to 2022.

Trajectory clustering analysis can be utilized to determine the main migration path of pollutants in the receptor station; however, the relative contribution level of the potential source area cannot be identified and simulated (Wang et al., 2017; Yerramilli et al., 2012). Further research is required to investigate the potential sources of PSCF and CWT methods, to obtain a better understanding of the long-range transport of pollutants to the Elk site, and to find potential source areas. Figure 6 and 7 show the calculation results of the WPSCF and WCWT of PM_{10} across the four seasons in Elk, respectively. WPSCF values of 0.1 – 0.3, 0.3 – 0.5, 0.5 – 0.7 and ≥ 0.7 were divided into very light, light, moderate, and severe pollution grids, respectively, to identify potential source grid attributes. The colors represent the contribution levels of the potential source area, and the red color could be associated with high concentrations (i.e., where the main potential sources were concentrated), whereas the blue color represents low concentrations (i.e., secondary potential sources).

In general, the spatial distributions of PM_{10} potential source areas and WPSCF and WCWT values were large in winter and spring, and lowest in summer and autumn. In winter, the main potential source areas contributing to high PM_{10} concentrations in Elk, with WPSCF values (≥ 0.7), were located in southwestern Poland, eastern Czech Republic, large areas of Slovakia, and north of Hungary. In these regions, the WCWT values were (≥ 50 μg/m³) (Fig. 6a and

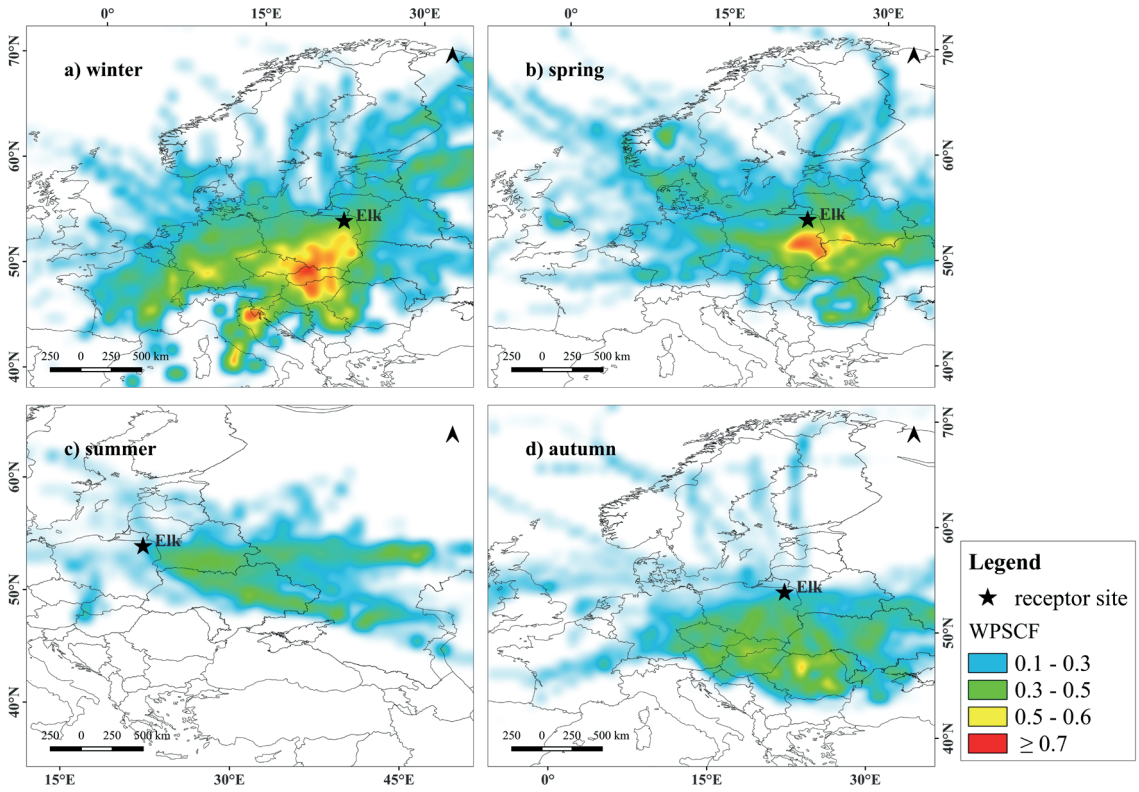

Fig. 6. Weighted Potential Source Contribution Function (WPSCF) map for PM_{10} from January 2021 to December 2022. The red color represents the high probable potential sources of extreme PM_{10} (over 90th percentile) while the blue color represents the low probable

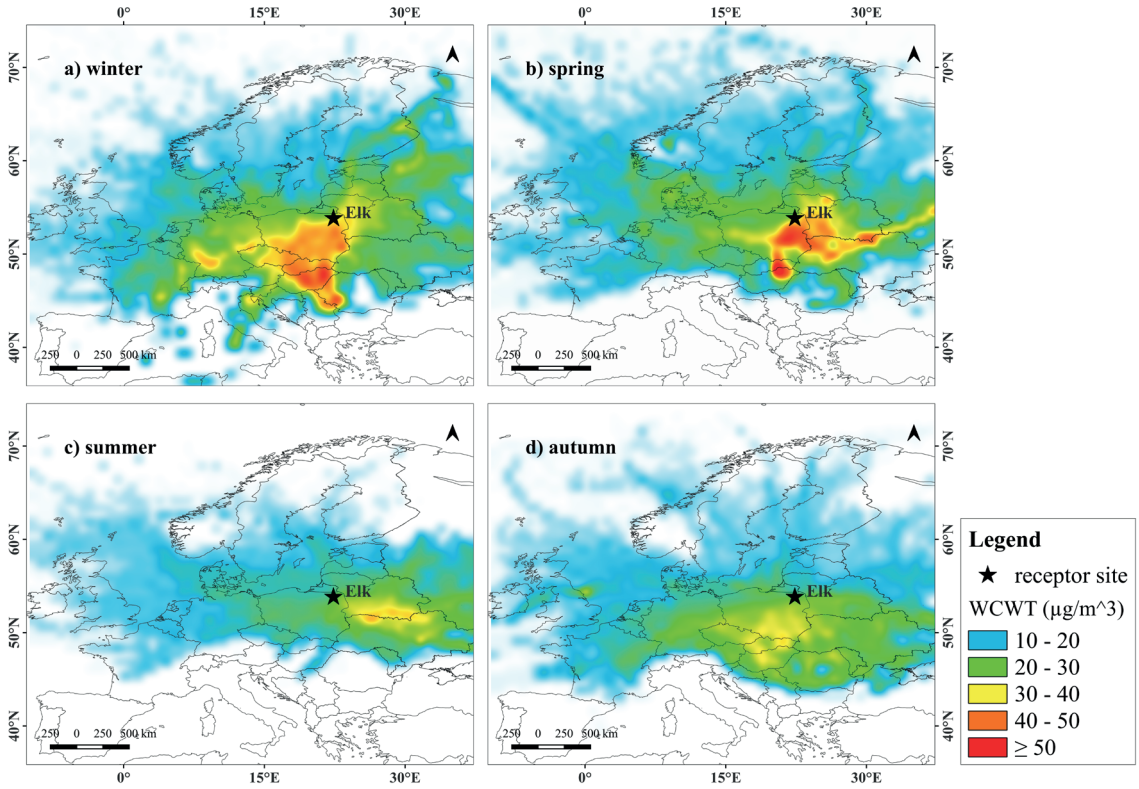

Fig. 7. Weighted Concentration-weighted Trajectories (WCWT) map for PM_{10} from January 2021to December 2022

7a). According to the European Environment Agency (EEA), the air quality in these regions has been found to exceed the limit values for PM_{10} concentrations in the air, as this region is highly industrialized, with a high concentration of coal-fired power plants and other sources of air pollution.

In spring, compared with winter, the main potential source areas of PM_{10} moved eastward, and the severe pollution source areas with high WPSCF values (≥ 0.7) were more concentrated in local areas south of the Elk site in east-central Poland (Mazovia Province). High WCWT values were mainly observed at ≥ 50 µg/m^3 in local areas south of the Elk site and the west of Belarus and northwest Ukraine, and some distributions in eastern Slovakia and northern Hungary. In summer, the spatial distributions of PM_{10} were mainly light polluted grids, with low WPSCF values of 0.1–0.5, and corresponding WCWT values (30–40 µg/m^3), associated

with south-eastern air masses, were mainly concentrated in the south of Belarus, southeast of Ukraine and small distributions in southern Russia in the North Caucasus (Fig. 6c and 7c). In autumn, the light and moderate pollution source areas of PM_{10} were concentrated in southeastern Poland and some individual distributions over Slovakia and Hungary (Central Transdanubia and Southern Transdanubia provinces) with WCWT values between (30 and 40 μg/m^3) (Fig. 7d).

CONCLUSIONS

In this study, cluster trajectory, Potential Source Contribution Function (PSCF), and Concentration-Weighted Trajectory (CWT) methods were used to identify potential source regions that could potentially affect a given PM_{10} measurement site in southeastern Baltic (Elk site).

The annual average of PM_{10} at the Elk site for the years 2021 and 2022 was 20.6 μg/m^3 and 19.6 μg/m^3, respectively, which are less than twice the EU standard. The PM_{10} mass showed seasonal variation, with a peak in winter and trough in summer. The high PM_{10} monthly mean values were related to heating in winter and peaked in March (31.7 μg/m^3). Conversely, the minimum monthly mean value of PM_{10} was observed in September at 13.7 μg/m^3.

Cluster analysis showed that the Elk atmosphere was mainly influenced by air masses from the western and southwestern directions. In addition, it was found that the main potential source regions contributing to high PM_{10} in winter are located in southwestern Poland and large areas of the Czech Republic and Slovakia, with WPSCF values ≥ 0.7, and corresponding WCWT values ≥ 50 μg/m^3. In spring, the main potential source areas of PM_{10} moved eastward, and high WPSCF and WCWT values were observed mainly in localized areas south of Elk in east-central Poland and northwestern Ukraine, with WPSCF values of ≥ 0.5 and WCWT values of 50 μg/m^3. In contrast, The WPSCF and WCWT values were low in summer and autumn, and the Elk site was less affected by the long-range transport.

In the future, we will conduct a case study and focus specifically on a high PM event in the southeastern Baltic region. In-depth research will also be conducted on how meteorological factors, such as temperature, wind speed, and relative humidity, affect PM concentrations.

REFERENCES

Bari A., Dutkiewicz V.A., Judd C.D., Wilson L.R., Luttinger D. and Husain L. (2003). Regional sources of particulate sulfate, SO2, PM2.5, HCl, and HNO3, in New York, NY. Atmospheric Environment, 37(20), 2837–2844. doi: 10.1016/S1352-2310(03)00200-0

Bihałowicz J.S., Rogula-Kozłowska W. and Krasuski A. (2021). Contribution of landfill fires to air pollution – An assessment methodology. Waste Management, 125, 182–191. doi: 10.1016/J.WASMAN.2021.02.046

Bodor Z., Bodor K., Keresztesi Á. and Szép R. (2020). Major air pollutants seasonal variation analysis and long-range transport of PM10 in an urban environment with specific climate condition in Transylvania (Romania). Environmental Science and Pollution Research International, 27(30), 38181. doi: 10.1007/S11356-020-09838-2

Byčenkiene S., Dudoitis V. and Ulevicius V. (2014). The Use of Trajectory Cluster Analysis to Evaluate the Long-Range Transport of Black Carbon Aerosol in the South-Eastern Baltic Region. Advances in Meteorology, 2014. doi: 10.1155/2014/137694

Draxler R.R. and Hess G.D. (1998). OverviewHYSPLIT4. Aust. Meteor. Mag., 47, 295–308.

Daly A. and Zannetti P. (2007). An Introduction to Air Pollution-Definitions, Classifications, and History. Retrieved from http://www.arabschool.org.sy

Dimitriou K., Grivas G., Liakakou E., Gerasopoulos E. and Mihalopoulos N. (2021). Assessing the contribution of regional sources to urban air pollution by applying 3D-PSCF modeling. Atmospheric Research, 248, 105187. doi: 10.1016/J.ATMOSRES.2020.105187

Fleming Z.L., Monks P.S. and Manning A.J. (2012). Review: Untangling the influence of air-mass history in interpreting observed atmospheric composition. Atmospheric Research, 104–105, 1–39. doi: 10.1016/J.ATMOSRES.2011.09.009

Heffter J.L., Taylor A.D. and Ferber G. (1975). A regional-continental scale transport, diffusion, and deposition model. Retrieved from https://repository.library.noaa.gov/view/noaa/14895

Hopke P.K., Barrie L.A., Li S.M., Cheng M.D., Li C. and Xie Y. (1995). Possible sources and preferred pathways for biogenic and non-sea- salt sulfur for the high Arctic. Journal of Geophysical Research, 100(D8). doi: 10.1029/95JD01712

Hsu, C. Y., Chiang, H. C., Chen, M. J., Yang, T. T., Wu, Y. S., & Chen, Y. C. (2019). Impacts of hazardous metals and PAHs in fine and coarse particles with long-range transports in Taipei City. Environmental Pollution, 250, 934–943. doi: 10.1016/J.ENVPOL.2019.04.038

Hsu Y.K., Holsen T.M. and Hopke P. K. (2003). Comparison of hybrid receptor models to locate PCB sources in Chicago. Atmospheric Environment, 37(4), 545–562. doi: 10.1016/S1352-2310(02)00886-5

Indumali U. and Appuhamillage W. (2018). THE IMPACT OF LIVING WALLS IN THE REDUCTION OF ATMOSPHERIC PARTICULATE MATTER POLLUTION.

Jasiński R., Galant-Gołębiewska M., Nowak M., Kurtyka K., Kurzawska P., Maciejewska M. and Ginter M. (2021). Emissions and Concentrations of Particulate Matter in Poznan Compared with Other Polish and European Cities. Atmosphere 2021, Vol. 12, Page 533, 12(5), 533. doi: 10.3390/ATMOS12050533

Kim D.S. (2013). Air Pollution History, Regulatory Changes, and Remedial Measures of the Current Regulatory Regimes in Korea. Journal of Korean Society for Atmospheric Environment, 29(4), 353–368. doi: 10.5572/KOSAE.2013.29.4.353

Kobza J., Geremek M. and Dul L. (2018). Characteristics of air quality and sources affecting high levels of PM10 and PM2.5 in Poland, Upper Silesia urban area. Environmental Monitoring and Assessment, 190(9), 1–13. doi: 10.1007/S10661-018-6797-X/TABLES/5

Li C., Dai Z., Liu X. and Wu P. (2020). Transport Pathways and Potential Source Region Contributions of PM2.5 in Weifang: Seasonal Variations. Applied Sciences 2020, Vol. 10, Page 2835, 10(8), 2835. doi: 10.3390/APP10082835

Li M., Huang X., Zhu L., Li J., Song Y., Cai X. and Xie S. (2012). Analysis of the transport pathways and potential sources of PM10 in Shanghai based on three methods. Science of The Total Environment, 414, 525–534. doi: 10.1016/J.SCITOTENV.2011.10.054

Ma Y.F., Du B.Y., Wang Q., Hu Q.Q., Bian Y.S., Wang M.B. and Jin S.Y. (2019). Analysis of the atmospheric pollution transport pathways and sources in Shenyang, based on the HYSPLIT model. IOP Conference Series: Earth and Environmental Science, 351(1), 012030. doi: 10.1088/1755-1315/351/1/012030

Majewski G., Rogula-Kozłowska W., Rozbicka K., Rogula-Kopie, P., Mathew, B. and Brandyk A. (2018). Concentration, Chemical Composition and Origin of PM1: Results from the First Long-term Measurement Campaign in Warsaw (Poland). Aerosol and Air Quality Research, 18(3), 636–654. doi: 10.4209/AAQR.2017.06.0221

Manisalidis I., Stavropoulou E., Stavropoulos A. and Bezirtzoglou E. (2020). Environmental and Health Impacts of Air Pollution: A Review. Frontiers in Public Health, 8, 505570. doi: 10.3389/FPUBH.2020.00014/BIBTEX

Moody J.L. and Galloway J.N. (2017). Quantifying the relationship between atmospheric transport and the chemical composition of precipitation on Bermuda. Tellus B: Chemical and Physical Meteorology, 40(5), 463–479. doi: 10.3402/tellusb.v40i5.16014

Nazar, W., Niedoszytko, M. (2022). Air Pollution in Poland: A 2022 Narrative Review with Focus on Respiratory Diseases. International Journal of Environmental Research and Public Health, 19(2), 895. doi: 10.3390/IJERPH19020895

Pouyaei A., Choi Y., Jung J., Sadeghi B. and Han Song C. (2020). Concentration Trajectory Route of Air pollution with an Integrated Lagrangian model (C-TRAIL Model v1.0) derived from the Community Multiscale Air Quality Model (CMAQ Model v5.2). Geoscientific Model Development, 13(8), 3489–3505. doi: 10.5194/GMD-13-3489-2020

Reizer M. and Orza J.A.G. (2018). Identification of PM10 air pollution origins at a rural background site. E3S Web of Conferences 28, Air Protection in Theory and Practice. doi: 10.1051/e3sconf/20182801031

Sahu S.K., Zhang H., Guo H., Hu J., Ying Q. and Kota S.H. (2019). Health risk associated with potential source regions of PM 2.5 in Indian cities. Air Quality, Atmosphere and Health, 12(3), 327–340. doi: 10.1007/S11869-019-00661-4/FIGURES/7

Shukurov K. and Shukurova L.M. (2017). Potential sources of Southern Siberia aerosols by data of AERONET site in Tomsk, Russia. 208. doi: 10.1117/12.2287936

Sirois A. and Bottenheim J.W. (1995). Use of backward trajectories to interpret the 5-year record of PAN and O3 ambient air concentrations at Kejimkujik National Park, Nova Scotia. Journal of Geophysical Research: Atmospheres, 100(D2), 2867–2881. doi: 10.1029/94JD02951

Stein A.F., Draxler R.R., Rolph G.D., Stunder B.J.B., Cohen M.D. and Ngan F. (2015a). Noaa's hysplit atmospheric transport and dispersion modeling system. Bulletin of the American Meteorological Society, 96(12), 2059–2077. doi: 10.1175/BAMS-D-14-00110.1

Stohl A. (1998). Computation, accuracy and applications of trajectories—A review and bibliography. Atmospheric Environment, 32(6), 947–966. doi: 10.1016/S1352-2310(97)00457-3

Wang S., Yu S., Li P., Wang L., Mehmood K., Liu W., Yan R. and Zheng X. (2017). A Study of Characteristics and Origins of Haze Pollution in Zhengzhou, China, Based on Observations and Hybrid Receptor Models. Aerosol and Air Quality Research, 17, 513–528. doi: 10.4209/aaqr.2016.06.0238

Wang S., Yu S., Yan R., Zhang Q., Li P., Wang L., Liu W. and Zheng X. (2017). Characteristics and origins of air pollutants in Wuhan, China, based on observations and hybrid receptor models. Http://Dx.Doi.Org/10.1080/10962247.2016.1240724, 67(7), 739–753. doi: 10.1080/10962247.2016.1240724

Wang Y.Q., Zhang X.Y. and Arimoto R. (2006). The contribution from distant dust sources to the atmospheric particulate matter loadings at Xian, China during spring. The Science of the Total Environment, 368(2–3), 875–883. doi: 10.1016/J.SCITOTENV.2006.03.040

Wang Y., Zhang X. and Draxler R.R. (2009). TrajStat: GIS-based software that uses various trajectory statistical analysis methods to identify potential sources from long-term air pollution measurement data. Environmental Modelling & Software, 24, 938–939. doi: 10.1016/j.envsoft.2009.01.004

Xin Y., Wang G. and Chen L. (2016). Identification of Long-Range Transport Pathways and Potential Sources of PM10 in Tibetan Plateau Uplift Area: Case Study of Xining, China in 2014. Aerosol and Air Quality Research, 16, 1044–1054. doi: 10.4209/aaqr.2015.05.0296

Yang H. and Smyntek P. (2014). Use of the mercury record in Red Tarn sediments to reveal air pollution history and the implications of catchment erosion. Environmental Science. Processes & Impacts, 16(11), 2554–2563. doi: 10.1039/C4EM00334A

Yerramilli A., Dodla V.B.R., Challa V.S., Myles L.T., Pendergrass W.R., Vogel C.A., Dasari H.P., Tuluri F., Baham J.M., Hughes R.L., Patrick C., Young J.H., Swanier S.J. and Hardy M.G. (2012). An integrated WRF/HYSPLIT modeling approach for the assessment of PM2.5 source regions over the Mississippi Gulf Coast region. Air Quality, Atmosphere and Health, 5(4), 401–412. doi: 10.1007/S11869-010-0132-1/TABLES/6

Zaręba M. and Danek T. (2022). Analysis of Air Pollution Migration during COVID-19 Lockdown in Krakow, Poland. Aerosol and Air Quality Research, 22(3), 210275. doi: 10.4209/AAQR.210275

Zhu L., Huang X., Shi H., Cai X. and Song Y. (2011). Transport pathways and potential sources of PM_{10} in Beijing. Atmospheric Environment, 45, 594–604. doi: 10.1016/j.atmosenv.2010.10.040